ELSEVIER

International Journal of Mass Spectrometry 207 (2001) 57–67

International Journal of Mass Spectrometry

Dynamic ion trapping in a cylindrical open cell for Fourier transform ion cyclotron resonance mass spectrometry

Vladimir Frankevich and Renato Zenobi*

Department of Chemistry, Swiss Federal Institute of Technology (ETH), Universitätstrasse 16, CH-8092 Zürich, Switzerland

Received 27 September 2000; revised 7 December 2000; accepted 11 December 2000

Abstract

Dynamic ion trapping is demonstrated for a Fourier transform ion cyclotron mass spectrometer with an open cylindrical cell. We show experimentally several features of dynamic ion trapping in the open cell: (a) ions can be selectively trapped in different regions of the cell, (b) mass selective accumulation of ions can be performed inside the trapping cylinder, (c) ions can be sequentially transferred between different regions of the cell, and (d) both positive and negative ions may be trapped and detected simultaneously. (Int J Mass Spectrom 207 (2001) 57–67) © 2001 Elsevier Science B.V.

Keywords: FT ICR; Trapped ion cells; Open cell; Dynamic trapping

1. Introduction

Numerous efforts in Fourier transform ion cyclotron resonance mass spectrometry (FTICR MS) [1] have been directed toward development and testing of FTICR cells of different geometries and configurations [2].

In its simplest configuration, ICR cell consists of six electrodes of equal size arranged in a cubic geometry [3]. All other cell geometries such as cylindrical traps, hyperbolic or Penning traps, screened ion traps, end cap–segmented ion cells, matrix shimmed traps, and open traps were designed to improve the capabilities of the cubic cell design for particular applications [4–8]. In spite of the different design and geometry, all traps with two end caps have in common a single potential well between the trap electrodes where ions are trapped by the combination of a strong axial magnetic field and a static axial electric field.

The concept of the open ICR cell is based on early experiments with electron and antiproton confinement for high-precision experiments [9]. In the open-cell configuration, the end cap electrodes are replaced with open cylinders. This improves the pumping efficiency, simplifies introduction and ejection of the charge particles, and eliminates the effect of charging and contamination of the trapping plates. Byrne and Farago have used an open cell to produce polarized electron beams [10]. DeGrassie and Malmberg confined an electron plasma by using three cylindrical electrodes [11,12]. It has been shown that the great advantage of the open–end cap electrode configuration is the easy access to the interior of the trap, which facilitates loading of particles and introducing micro-

*Corresponding author. E-mail: zenobi@org.chem.ethz.ch

PII S1387-3806(01)00365-7

waves or laser beams. The open-cell design for FTICR MS developed by Laude [8,13] permits efficient ion trapping and detection. This design enhances FTICR MS capabilities in many applications where the physical presence of the trapping electrodes is impossible or complicates the experimental procedure. Open-cell arrangements have been widely utilized in FTICR mass spectrometers having external ion sources in order to increase ion injection efficiency and eliminate ion trajectory perturbation from ions that pass through the trapping electrode conductance limit [13–15].

Applying a conventional static electric potential to each trapping electrode may trap only positive or negative ions. Simultaneous storage of positive and negative ions in a static electric field is possible in a double-well potential. It can be created with additional electrodes. Wang and Wanczek [16] have used shielding grids in front of the trapping plates to create a special potential well for simultaneous trapping of positive and negative ions. Vartanian and Laude introduced additional rings in the open-cell design to create several potential wells (a "nested" trap) for positive and negative ion trapping [17]. The rings are alternately set to positive or negative potential. A cylindrical cell with segmented trap electrodes, consisting of two concentric rings, was also used to trap ions of both charges [18].

Positive and negative ions are stored in different regions of the cell in those experiments. However, in many cases, for example, ion/ion interaction studies, the ions have to share the same region of the cell. The use of static electric field for ion trapping lacks such a capability.

Alternatively, in a quadrupolar ion trap (ITMS), both positive and negative ions may be trapped simultaneously in the same region. Although only positive or negative ions can be detected in a common mode of operation [19], a Fourier-transformed detection of the image current in a quadrupole ion trap [20,21] gives a possibility for simultaneous detection of positive and negative ions.

Gorshkov et al. experimentally demonstrated that ion trapping in a FTICR MS may be achieved by using a RF electrical field applied to the trapping electrodes of standard cubic cell [22]. The use of RF rather than DC voltage for ion trapping in FTICR MS has been called dynamic trapping to distinguish it from static trapping of ions of a single charge sign. Simultaneous trapping and detection of positive and negative ions has been demonstrated. The method was further enhanced by using a circularly polarized excitation, which makes it possible to distinguish positive and negative ions trapped simultaneously [23]. Wang and Wanczek also suggested that ions of both charge signs could be trapped in ICR by applying a RF electric quadrupolar potential [24]. Also, an RF electric quadrupole potential has been applied to FTICR by Rempel and Gross for high-pressure collisional stabilization of reaction intermediates and products [25].

Although virtually most of the FTICR experiments have been performed with static trapping, even the nearly quadrupolar electrostatic trapping potential of a hyperbolic trap [26] presents several experimental difficulties [27,28].

The method of dynamic trapping is characterized by simplicity of the experimental setup, high efficiency of ion storage, and the possibility of using RF fields of low amplitude and frequency.

In this work, we experimentally demonstrate dynamic ion trapping in an open FTICR cell. It is shown that all prior capabilities and advantages of the open-cell design are preserved. We demonstrate several features of dynamic trapping in open cell: (a) ions can be selectively trapped in a different regions of the cell; (b) mass selective accumulation of ions can be performed inside the trapping cylinder; (c) ions can be sequentially transferred between different regions of the cell; and (d) both positive and negative ions may be trapped and detected simultaneously.

Some of the features of the open cell with dynamic trapping are similar to dual and multipole trap experiments [29–31]. The manipulation developed and demonstrated includes the mass selective ion transfer between the trap cylinders and the detection at the central region of the trap and mass selective accumulation of externally produced ions in one of the trap cylinder.

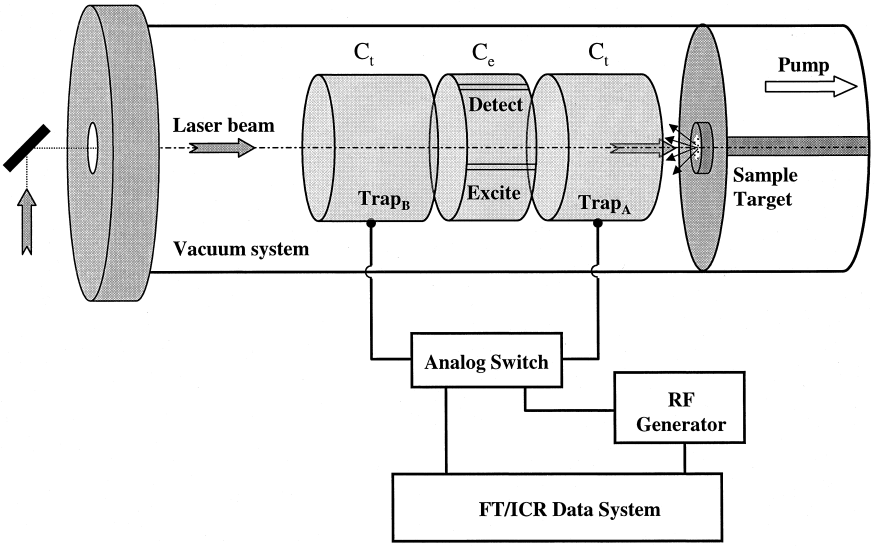

Fig. 1. Schematic illustration of the open FTICR cell developed in this work and used for MALDI experiments and associated circuitry. C_t=40 mm, C_e=30 mm (aspect ratio 1.4).

2. Experimental

Experiments were performed on a Fourier transform ion cyclotron resonance (FTICR) mass spectrometer that consists of a home-built vacuum system with a 4.7-Tesla superconducting magnet (Bruker, Fällanden, Switzerland) and an Odyssey data acquisition system (Finnigan FT/MS, Madison, WI). A home-built cylindrical open cell with C_t = 40 mm, C_e = 30 mm, d = 60 mm, and an aspect ratio of 1.4 was used for dynamic trapping of MALDI ions (Fig. 1). The instrument has an internal MALDI source located at the low-pressure region a few millimeters away from the ICR cell. For laser desorption, a Nd:YAG laser (Continuum, Minilite ML-10, Santa Clara, CA, USA) operated at 355 nm was employed. Laser desorption/ionization was accomplished at a pulse energy of ~20 μJ. Reference ions were produced from a single laser shot and trapped by applying a 10-Vpp AC voltage produced by an external function generator (Tabor 8551, Tabor Electronics Ltd., Israel), which can synthesize sinusoidal, triangle, and rectangular waveforms at frequencies up to 50 MHz, with an amplitude up to 15 Vpp. If necessary, a conventional static potential can be applied to the trapping cylinders using a home-built switch box (Fig. 1). The MALDI sample was placed in the main chamber and positioned ~15 mm from one edge of the trapping cylinder. MALDI samples were prepared using the standard dried-droplet method. 2,5-dihydroxy benzoic acid (DHB) matrix was purchased from Fluka (Buchs, Switzerland); the dinucleotide AG was obtained from Sigma (Buchs, Switzerland). Aqueous stock solutions were prepared. The reference ions drift into the cell and become trapped in the RF field. After an appropriate reaction delay period, analyte ions were excited by chirp excitation and detected. For each measurement, 50 scans were co-added. The 32 K of raw data was Fourier transformed and displayed in magnitude mode. Gated trapping was used for conventional DC trapping experiments. The typical pressure in the cell region was 5×10^{-9} Torr.

3. Results and discussion

3.1. Open-cell design

The aspect ratio for the conventional closed ICR cell is simply defined as a ratio of the cell length and the cell diameter. From SIMION calculations of the

electric field distribution inside the ICR cell, the aspect ratio for the open cell can be expressed as [32]:

$$R = 1.19\ (C_t + C_e)/d, \quad (1)$$

where C_t is the length of the trap cylinders, C_e is the length of the excitation/detection cylinder, and d is the trap diameter.

The potential well depth and radial electric field inside the cell depend strongly on the value of the aspect ratio [8,32]. An open cell with an aspect ratio of 1.4 was built for our experiments ($C_t = 40$ mm, $C_e = 30$ mm, and $d = 60$ mm) because for this fixed cell volume ($2C_t + C_e = \text{Const}$), the potential well depth was found to be maximum at a low radial electric field. The experimentally measured ion cyclotron frequency shift for the open cell used in this work is 13 Hz/V.

3.2. DC trapping in the open-cell experiment

The potential distribution in the open cell is shown in Fig. 2(a). The centerline trap potential profile (trapping potentials were set to +5 V) was obtained from SIMION calculations. Positive ions with an energy of up to 4 V can be trapped in the center region of the cell when DC trapping potential is applied. A negative DC potential is used to obtain mass spectra of negative ions.

The experimental sequence for the static DC trapping includes ion introduction, gated trapping, excitation, and detection. Spectra of positive and negative DHB ions, as well as the negative ion spectrum of DHB+AG were obtained for comparison with other types of experimental measurements.

3.3. Dynamic trapping in the open cell

Fig. 2(b) shows the centerline potential distribution when a ±5 V RF field was used for ion trapping. The trap potential has the same shape as in Fig. 2(a) but inverts periodically at the frequency of the RF trapping field, Ω. The grounded sample target from one side and the cell flange from the other serve as additional trap electrodes. There are three potential wells where ions can be trapped: two of them are

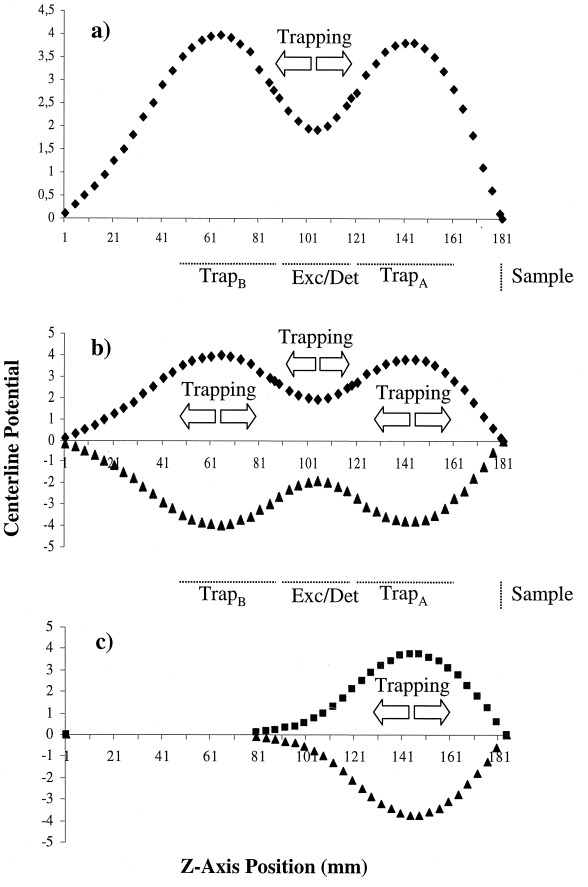

Fig. 2. SIMION plot of the potential well depth versus *Z*-axis position for the open cell (aspect ratio 1.4, Excite/Detect potentials = 0 V). (a) DC trapping (trap potentials +5 V): ions are trapped only in the center region of the cell. (b) Dynamic trapping (RF potential 5 Vpp is applied to both of the trap cylinders): ions can be trapped in three regions of the cell. (c) Dynamic trapping (RF potential 5 Vpp is applied to Trap$_A$ cylinder): ions can be trapped in one of the cell cylinder.

inside the trap cylinders (Trap$_A$ and Trap$_B$), and one is at the center of the cell (Excite/Detect region).

The ability to trap ions by alternating electric fields of low amplitude and frequency follows from an understanding of the ion motion in an RF field. It has been shown that in the quadrupolar approximation of the trapping electric filed inside the ICR ion trap, the ion motion can be described by the following equation [22]:

$$Z'' + 2\gamma Vz/m \cos(\Omega t) = 0, \quad (2)$$

where V is the amplitude of the RF voltage applied to each end cap and γ is determined by the trap geometry.

Eq. (2) is a form of the well-known Mathieu equation [33] with a stability parameter q_z, which can be expressed as:

$$q_z = 4\gamma Vz/m\Omega^2. \quad (3)$$

Because of the presence of the strong magnetic field in Z direction, the ion motion in radial direction is stable and only Z motion needs to be considered. Once ions are stable in the Z direction, their trajectories are confined inside the cell. Frequency and amplitude of the RF field should satisfy the value of q_z at which the ion motion is stable [34]:

$$0 < q_z < 0.9 \quad (4)$$

In our experiment, the ion motion inside the trap for an ion with $m/z = 100$ Da at an RF field amplitude of 10 Vpp and a frequency of >20 kHz is stable according to Eq. (4). Although the previous theory was derived for the cubic ICR cell geometry [22], we found experimentally that it also describes the open-cell well. Because of the different size and potential distribution of the central region and the trap cylinders, the trapping conditions there are different. Experimentally, it was found that

$$(1/m\Omega^2)_{\mathrm{Trap_A}} = 1.46(1/m\Omega^2)_{\mathrm{Central}};\ (\gamma_{\mathrm{A}} = 1.46\gamma_{\mathrm{Central}}) \quad (5)$$

Fig. 3(a) illustrates the experimental FTICR sequence used for dynamic trapping in the open cell. An RF trapping potential (10 Vpp, 10–100 kHz sinusoidal waveform) was applied to both trap cylinders ($\mathrm{Trap_A}$ and $\mathrm{Trap_B}$) during introduction and accumulation periods. Ions of both charge signs with masses corresponding to the stability region (Eqq. [3] and [4]) were trapped in three regions of the open cell: both of the trap cylinders ($\mathrm{Trap_A}$ and $\mathrm{Trap_B}$) and the center region (Excite/Detect). Only positive ions were excited and detected when a positive DC offset (dashed line on Fig. 3[a]) is applied to the trap cylinders, and only negative trapped ions were detected for negative DC offset (solid line on Fig. 3[a]).

Simultaneous excitation and detection of the ions of both charge signs is possible when no DC offset or the same RF potential are still present during excitation and detection events. This may induce unfavorable noise in the detection circuit, although the RF trapping frequency is generally much lower than the ion cyclotron frequency. However, in some cases (high mass detection), frequency filters were required to reduce the RF trapping field and its harmonics from the detection circuit.

3.4. Dynamic trapping in the first trapping cylinder

Ions can be trapped in one of the trapping cylinders as shown in Fig. 2(c). In this case, RF potential is applied to the $\mathrm{Trap_A}$ cylinder, whereas all other cylinders are at ground potential. The open trap can be approximated by a cylindrical trap with grounded end caps in this experiment. One end cap is the grounded sample target, and the other is a central cylinder. The SIMION plot in Fig. 2(c) shows that the potential well depth created by an alternating electric field inside the cylinder is deeper than the one created if RF is applied to both trap cylinders (Fig. 2[b]). It is caused by the trap electrodes geometry.

Once the ions are trapped in the first cylinder, they have to be moved into the central region of the trap for the excitation/detection events. The following experimental sequences were used for trapping and sequential ion transfer (Fig. 3[b]): An RF trapping potential is applied only to one trap cylinder ($\mathrm{Trap_A}$) during ion introduction and accumulation, while all others are kept at zero potential. After the appropriate ion accumulation period, ions are transferred from the first cylinder into the central region of the trap by applying an attractive potential to the second trap cylinder. Excitation/detection events are the same as discussed above. Positive ions, negative ions, or both can be excited and detected.

3.5. Selective trapping of ions

As follows from the previous discussion, there is a stability region defined by the ion's mass-to-charge ratio and the RF field amplitude and frequency (Eqq.

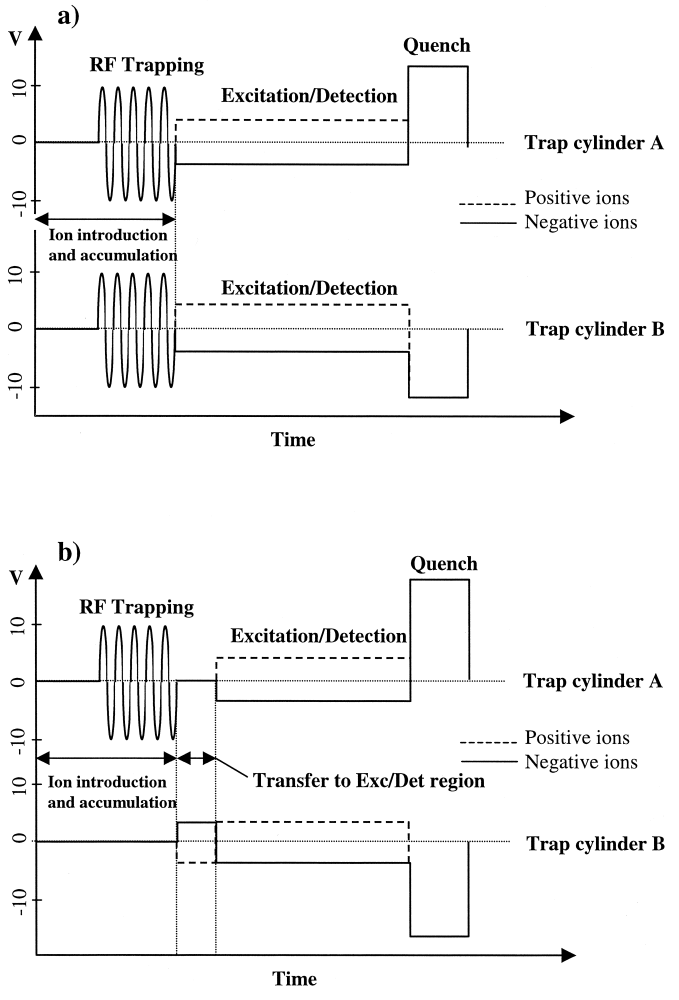

Fig. 3. FTICR event sequence for dynamic trapping of ions in an open cell. (a) Dynamic trapping in an open cell. (b)Dynamic trapping in a single cell cylinder.

[3] and [4]). This means that for a given mass-to-charge ratio, there is a minimum frequency (maximum amplitude) below which the ion motion inside the trap becomes unstable.

Fig. 4 illustrates the dependence of dynamically trapped negative ions on RF trapping frequency. Ions with three different masses produced from DHB and AG were investigated. The frequency of the RF trapping potential was varied while keeping the amplitude constant (V_{ac} = 10 V).

The plot on Fig. 4 gives the minimum frequency of the RF voltage by which the ions can be trapped. The optimum trapping frequency can also be obtained. The experimentally defined minimum trapping frequency for the different masses satisfies the Mathieu equation:

$$q_z = k/(m_1\Omega_1^2) = k/(m_2\Omega_2^2) = k/(m_3\Omega_3^2) = 0.9, \quad (6)$$

where k is defined in Eq. (3) and m_1 = 579, m_2 = 329, and m_3 = 153.

The minimum trapping frequency as a function of

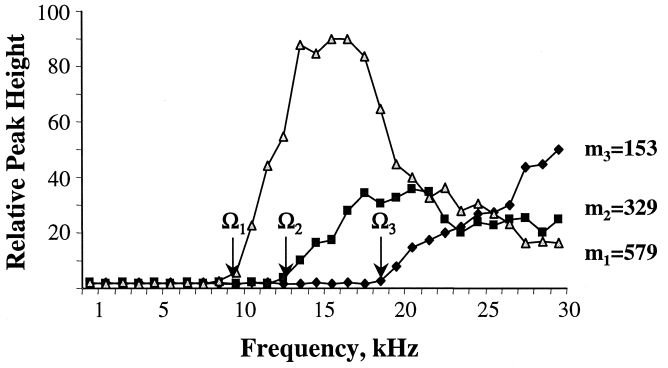

Fig. 4. Dependence of relative peak height of dynamically trapped negative ions on RF trapping frequency. Points Ω_1, Ω_1, and Ω_3 correspond the minimum RF frequency (trapping limits) for trapping ions at $m/z = 579$, $m/z = 329$, and $m/z = 153$.

mass for our cell geometry at a constant amplitude ($V_{ac} = 10$ V) can be empirically expressed as

$$\Omega_{min} = 235/m^{1/2}, \quad (7)$$

where Ω is in kHz and m is the mass-to-charge ratio in Th. This equation can be used for selective ion trapping in the open cell to define the cutoff trapping frequency.

The maximum trapping efficiency was obtained for $q_z = 0.4$, in a good agreement with nonmagnetic ion traps [33] and previous work on dynamic trapping in FTICR [22].

An example of selective trapping in the first cylinder is shown on Fig. 5. The spectrum of DHB matrix and AG collected using conventional DC trapping in the open cell is shown in Fig. 5(a). The peak of interest is the AG molecular ion at $m/z = 579$ Da with a signal-to-noise ratio of 30.

The spectrum in Fig. 5(b) shows the result obtained from an experiment with dynamic trapping in the first cylinder. An RF field with a frequency of 10 kHz was used for dynamic trapping. As follows from Eq. 6, all ions with masses <550 Da are lost from the trap because of unstable trajectories. There is a large increase in the signal-to-noise ratio and considerable increase in peak resolution. The resolution increase can be attributed to reduction in space charge because the low-mass ions are removed. This experiment shows that the analyte ions can be successfully separated from the matrix ions, which is important for MALDI-MS.

3.6. Dynamic accumulation of externally produced ions in the open cell

The method of dynamic trapping can be successfully used for the stepwise accumulation of low-abundance ions in one of the trap cylinders. This accumulation may be necessary for obtaining higher signal-to-noise ratios or for increasing the dynamic range. In this work, we consider the accumulation of MALDI ions produced from several laser shots. The accumulation of ions with gated trapping under low-pressure conditions is not effective. Ions are introduced into the cell while one of the trap potentials is lower than the other and become trapped when the potential is gated to create an appropriate potential well. For the next ion introduction, the potential should be lowered and gated again, and in the absence of an additional ion cooling mechanism, most of the previously accumulated ions will be lost. Fig. 6(a) presents experimental data for the ion loss from the open cell with DC trapping during the reintroduction of ions. The results were obtained for the deprotonated DHB molecular ion ($m/z = 153$) and low-pressure conditions. One of the trap potentials was gated from 0 to -2 volts during ion introduction. It can be seen that 90% of the trapped ions are lost

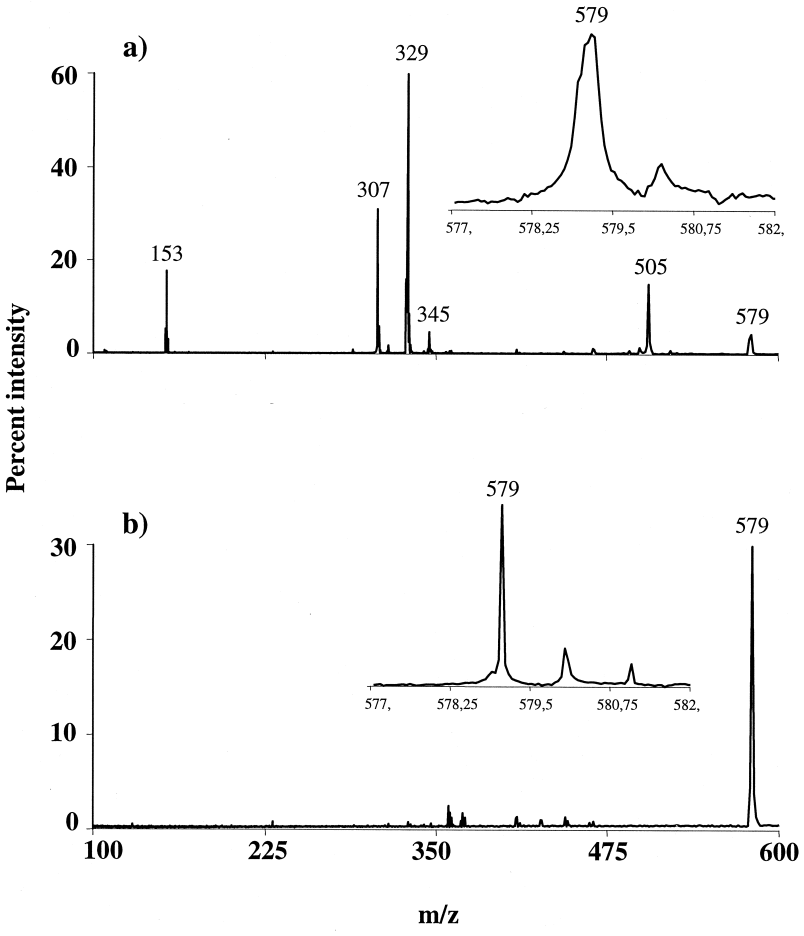

Fig. 5. Selective trapping of AG molecular ion in the first trapping cylinder. (a) static trapping; (b) dynamic trapping (10 Vpp, 12 kHz).

during the reintroduction period, and the accumulation efficiency may be calculated as:

$$(N_i)_{\mathrm{DC}} = (N_0)_{\mathrm{DC}}(1 + n + \ldots n^i), \quad (8)$$

where i is the number of ion introduction steps, N_0 the number of ions trapped from a single laser shot, and n the ion retention coefficient during the reintroduction (n=0.1). For four laser shots, $N_4 = 1.111N_0$. The accumulation efficiency for the DC trapping becomes higher when ion-neutral collisions take place in the trap. Note that by appropriate adjustment of the DC potentials during gated trapping, successful stepwise ion accumulation is possible in static trapping mode [31].

In the dynamic trapping mode, the ions may be introduced directly into the RF field and become trapped. Subsequent ion introduction will add additional ions to the previously trapped, that is:

$$(N_i)_{\mathrm{RF}} = i(N_0)_{\mathrm{RF}}. \quad (9)$$

Generally we observe that the primary trapping efficiency of dynamic trapping is lower (it is RF phase dependent) than in conventional DC trapping but the accumulation efficiency is higher.

The measured accumulation efficiencies for the deprotonated DHB molecular ion for DC and RF trapping are compared in Fig. 6(b). The primary trapping efficiency is almost two times higher for the DC trapping, but the accumulation efficiency is better for dynamic trapping. Ions can be successfully accu-

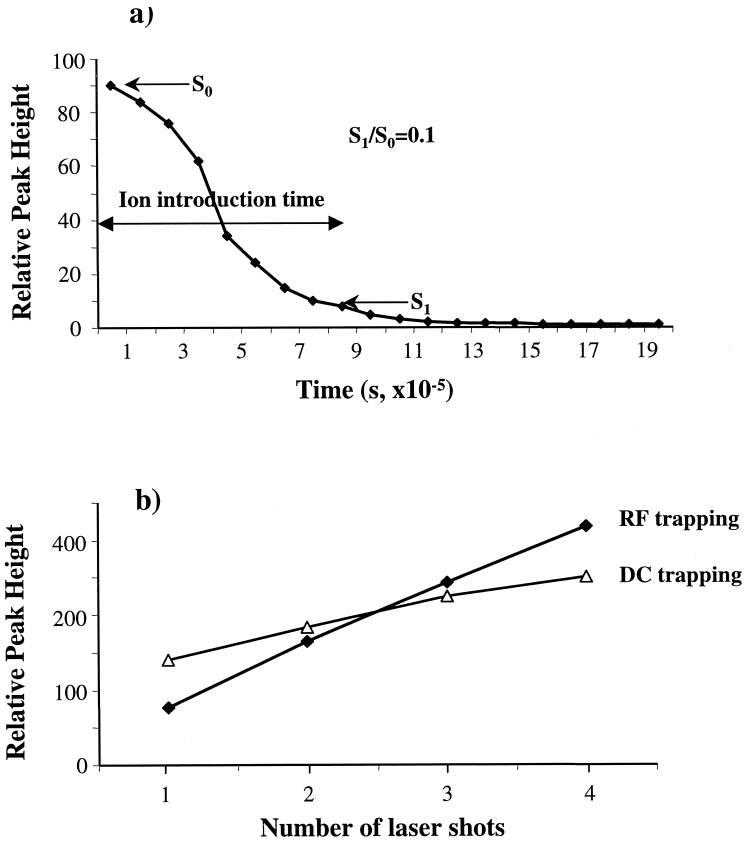

Fig. 6. (a) Ion loss from the open cell during the reintroduction as a function of time when the trap potential is 0. (DC gated trapping, *m/z*=153). (b) Accumulation efficiency for the DHB molecular ion (*m/z*=153) for DC and RF trapping.

mulated in the first cylinder and than transferred into the center trap for detection.

3.7. Simultaneous positive and negative ion detection

Successful dynamic trapping of DHB ions is shown in Fig. 7, with the RF trapping voltage at V_{ac} = 10 V and a trapping frequency of 75 kHz. In positive ion mode (DC trapping; Fig. 7[a]), peaks at *m/z* = 177, *m/z* = 199, and *m/z* = 273 are readily observed. In the negative ion mode (DC trapping, Fig. 7[b]), the only significant ionic species are *m/z* = 153 and *m/z* = 409. With dynamic trapping (Fig. 7[c]), with RF applied to both of the trap cylinders during introduction, accumulation, and excitation events, we detected all of the species observable in both static trapping modes, as well as a number of additional species. Some of them are probably caused by ion–ion and ion–electron reactions during simultaneous positive and negative ion trapping.

4. Conclusions and outlook

An FTICR cylindrical open cell with dynamic trapping of ions has been developed and experimentally evaluated. Several capabilities that should serve to extend the applications of FTICR have been demonstrated including trapping of ions inside the trap cylinders, which increases the cell capacity and dynamic range; selective trapping of ions allowing to separate ions during introduction and accumulation; mass selective ion transfer between the trap regions; mass selective accumulation of ions in one of the cylinder, which may

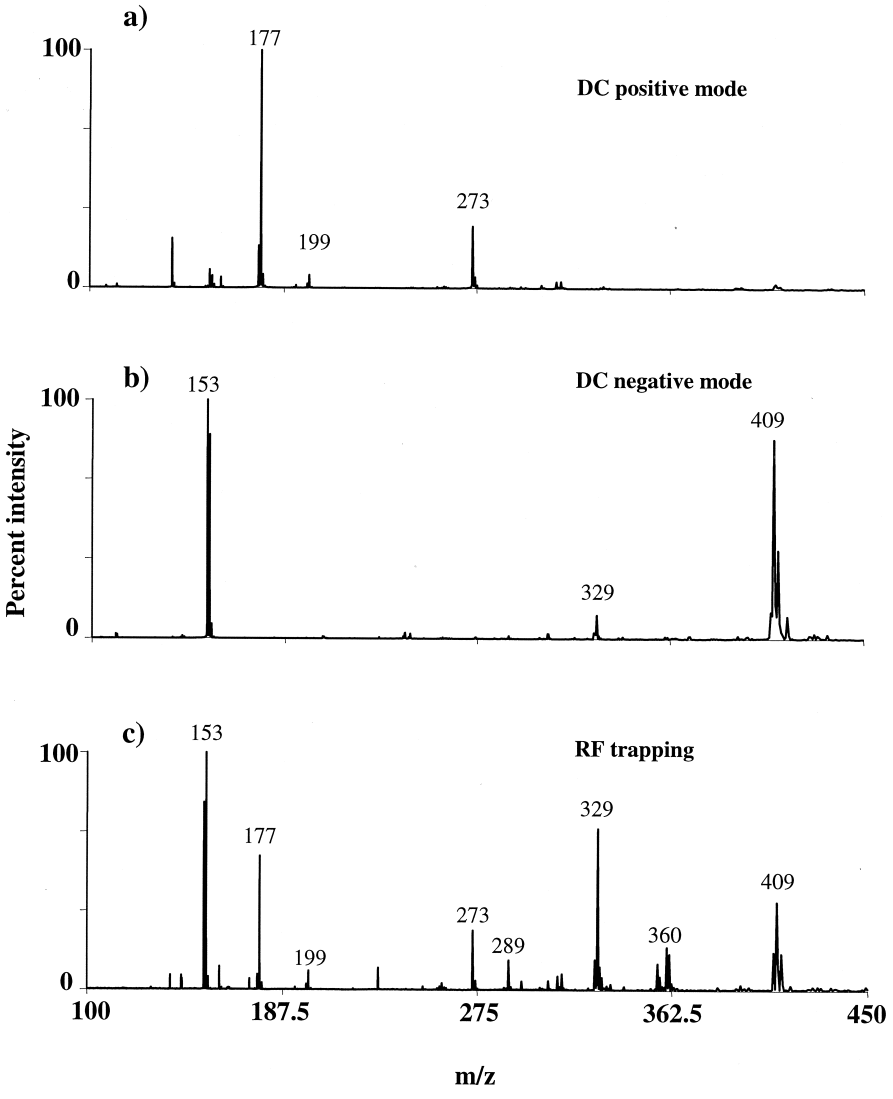

Fig. 7. Simultaneous positive and negative ion trapping. (a) static (DC) positive ion trapping mode; (b) static negative-ion trapping mode; (c) dynamic trapping (RF applied to both of the trap cylinders; 10 Vpp, 75 kHz).

be useful for obtaining higher signal-to-noise ratios or for increasing dynamic range; and simultaneous positive and negative ion detection, which gives in addition the possibilities of ion–ion reaction.

Acknowledgements

We thank Dr. Michael Gorshkov from the Institute of Energy Problems of Chemical Physics, Russian Academy of Sciences; Dr. Elizabeth Stevenson for help and useful discussions on the subject of this article; and Leo Weinberg for his help with electronic construction.

References

[1] M.B. Comisarow, A.G. Marshall, Chem. Phys. Lett. 25 (1974) 282.

[2] A.G. Marshall, C.L. Hendrickson, G.S. Jackson, Mass Spectrom. Rev. 17 (1998) 1.
[3] M.B. Comisarow, Int. J. Mass Spectrom. Ion Phys. 37 (1981) 251.
[4] S.H. Lee, K.P. Wanczek, H. Hartmann, Adv. Mass Spectrom. 8B (1980) 1645.
[5] D.L. Rempel, E.B. Ledford, S. Huang, M.L. Gross, Anal. Chem. 59 (1987) 2527.
[6] P. Caravatti, M. Allemann, Org. Mass. Spectrom. 26 (1991) 514.
[7] S. Guan, A.G. Marshall, Int. J. Mass Spectrom. Ion Processes 146/147 (1995) 261.
[8] S.C. Beu, D.A. Laude, Int. J. Mass Spectrom. Ion Processes 112 (1992) 215.
[9] G. Gabrielse, L. Haarsma, S.L. Rolston, Int. J. Mass Spectrom. Ion Processes, 88 (1989) 319.
[10] J. Byrne, P.S. Farago, Proc. Phys. Soc. 86 (1965) 801.
[11] J.S. deGrassie and J.H. Malmberg, Phys. Rev. Lett. 39 (1977) 1077.
[12] J.H. Malmberg, J.S. deGrassie, Phys Rev. Lett. 35 (1975) 577.
[13] S.C. Beu, D.A. Laude, Anal. Chem. 64 (1992) 177.
[14] J.A. Marto, S. Guan, A.G. Marshall, Rapid Commun. Mass Spectrom. 8 (1994) 615.
[15] S.C. Beu, M.W. Senko, J.P. Quinn, F.M. Wampler, F.M. McLafferty, J. Am. Soc. Mass Spectrom. 4 (1992) 557.
[16] Y. Wang, K.P. Wanczek, Rev. Sci. Instrum. 64 (1993) 883.
[17] V.H. Vartanian, D.A. Laude, Org. Mass Spectrom. 9 (1994) 692.
[18] R. Malek, K.P. Wanczek, Rapid Comm. Mass Spectrom. 11 (1997) 1616.
[19] G.C. Stafford, E.P. Kelley, J.E.P. Syka, W.E. Reynolds, J.F.J. Todd, Int. J. Mass Spectrom. Ion Processes 60 (1984) 85.
[20] V.E. Frankevich, M. Soni, M. Nappi, G. Cooks, US Patent 5,625,186 (1997).
[21] M. Soni, V. Frankevich, M. Nappi, R. Santini, J. Amy, G. Cooks, Anal. Chem. 68 (1996) 3314.
[22] M.V. Gorshkov, S. Guan, A.G. Marshall, Rapid Comm. Mass Spectrom. 6 (1992) 166.
[23] S. Guan, M.V. Gorshkov, A.G. Marshall, Chem Phys. Lett. 198 (1992) 143.
[24] Y. Wang, K.P. Wanczek, Proceedings of the 39th Annual Conference on Mass Spectrometry and Allied Topics, Nashville, TN, ASMS, East Lansing, MI, 1991, p. 1519.
[25] D.L. Rempel, M.L. Gross, Proceedings of the 39th Annual Conference on Mass Spectrometry and Allied Topics, Nashville, TN, ASMS, East Lansing, MI, 1991, p. 453.
[26] W.W. Win, M. Wang, A.G. Marshall, E.B. Ledford, J. Am. Soc. Mass Spectrom. 3 (1992) 188.
[27] E.B. Ledford, D.L. Rempel, M.L. Gross, Anal. Chem. 56 (1984) 2744.
[28] S.-P. Chen, M.B. Comisarow, Rapid Comm. Mass Spectrom. 6 (1991) 1.
[29] S. Guan, A.G. Marshall, J. Am. Soc. Mass Spectrom. 7 (1996) 101.
[30] D.P. Littlejohn, S. Ghadery, US Patent 4,581,533 (1986).
[31] M.V. Gorshkov, L. Pasa-Tolic, J.E. Bruce, G.A. Anderson, R.D. Smith, Anal. Chem. 69 (1997) 1307.
[32] V.H. Vartanian, D.A. Laude, Int. J. Mass Spectrom. Ion Processes 141 (1995) 189.
[33] R.E. March, J.F.J. Todd, Practical Aspects of Ion Trap Mass Spectrometry, CRC Press, New York, 1995, Vol. 1.
[34] R.E. March, R.J. Hughes, Quadrupole Storage Mass Spectrometry, Wiley, New York, 1989.